



## Operation of the ATLAS Semiconductor Tracker

---

**Nick Barlow\***

*for the ATLAS SCT Collaboration*

*University of Cambridge*

*E-mail: [nbarlow@hep.phy.cam.ac.uk](mailto:nbarlow@hep.phy.cam.ac.uk)*

ATLAS is one of the large general purpose detectors for the Large Hadron Collider at CERN, designed to search for a wide range of New Physics phenomena. In order to fulfil this design brief, a precise, fast, radiation-hard tracking system is essential. In this note I will describe the design and construction of the ATLAS Semiconductor Tracker (SCT), and will present some results from commissioning runs on cosmic ray data.



*9th International Conference on Large Scale Applications and Radiation Hardness of Semiconductor Detectors, RD09  
September 30-October 2, 2009  
Florence, Italy*

---

\*Speaker.

## 1. Introduction

The ATLAS [1] Inner Detector comprises three subsystems, each with a different role to play in the detection and measurement of charged particle tracks. All three subdetectors are located in a 2T solenoidal magnetic field, enabling transverse momenta of charged particle tracks to be measured. The Pixel detector is the innermost system, and is designed to locate vertices with extremely high precision. It also aids pattern recognition for track finding. The Transition Radiation Tracker (TRT) is a straw tube tracker, designed to provide a large number of position measurements per track, improving transverse momentum resolution, and is also useful for fast pattern recognition. In this note I will focus on the Semiconductor Tracker (SCT), a silicon strip detector situated between the Pixel and TRT detectors.

## 2. Design of the SCT

### 2.1 Requirements

The SCT was designed to fulfil the following requirements [2]:

- Reconstruct isolated leptons with  $p_T > 5\text{GeV}$  with 95% efficiency out to  $|\eta| < 2.5$ .
- Measure momentum with better than 30% precision even at  $p_T = 500\text{GeV}$ .
- Enable tracking back to the vertex  $z$ -coordinate with better than 1mm precision.
- Provide two-track resolution better than  $200\mu\text{m}$  at 30cm radius.
- Contribute no more than 20%  $X_0$  material in total.
- Be sufficiently radiation hard to withstand a fluence of  $2 \times 10^{14}\text{n/cm}^2$  (1MeV neutron equivalent)

### 2.2 Design

The SCT can be subdivided into barrel and endcap regions. The barrel section comprises four layers, covering a range  $|\eta| < 1$ , while each endcap consists of nine disks, extending the coverage over a range  $|\eta| < 2.5$ .

The basic unit for construction and readout is a *module*. There are 2112 modules in the barrel [3] and 968 in each endcap [4]. Figure 1 shows barrel and endcap modules. Each module is double-sided, with 768 strips per side, and a stereo angle of 40mrad between the direction of the strips on each side, to enable the detection of 3D “space points” when there are hits registered on strips on both sides of the module. The strip pitch is 80 microns for barrel modules, and in the range 57-94 microns for the endcap modules, where the strips fan out radially with respect to the beam axis.

The sensors are single-sided p-on-n strips, with an average depletion voltage of around 60V before radiation damage. The readout electronics are placed on a wrap-around hybrid, with six custom “ABCD” ASIC chips [5] per side (each chip reads out 128 strips).

A binary readout scheme is used, where a channel either registers a hit or does not, depending on whether the charge on that strip exceeds a programmable threshold.

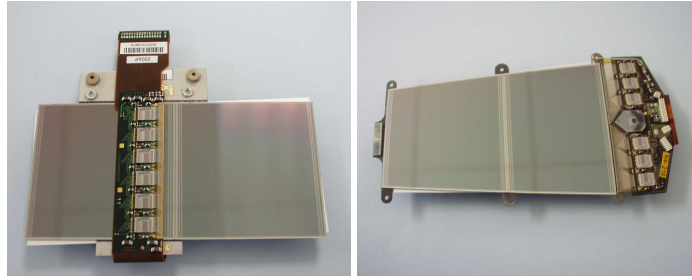


**Figure 1:** Barrel (left) and endcap (right) SCT modules.

### 2.3 Cooling

In order to minimize the effects of radiation damage, it is desirable to operate the SCT at a temperature between  $-10$  and  $0^{\circ}\text{C}$ . An evaporative cooling system was chosen, shared with the Pixel detector, and with  $\text{C}_3\text{F}_8$  as the coolant. In May 2008, a serious incident occurred when slippage of a magnetic clutch caused the cooling plant to overheat and fail. Sensors have since been installed to guard against similar malfunctions, and a further refurbishment in 2009 saw the installation of a larger coolant tank, and measures to mitigate against excessive vibration of the compressors. The plant has been operational almost full time since June 2009, and is working reliably, with only occasional down-time. The typical operating temperature of the modules is close to  $0^{\circ}\text{C}$ .

### 2.4 Optical communication

Communication between the SCT modules and the off-detector electronics is handled by optical fibre connections. Clock and command signals are sent from the “Back-Of-Crate” cards (BOCs) along “TX” fibres, of which there is one fibre per module, while data is returned to the BOC along “RX” fibres, one per module side. Both RX and TX links have a redundancy scheme in case of fibre breaks or transmitter failures. For the TX, it is possible for a module to receive clock and command signals electronically from a neighbouring module. For the RX, it is possible to read out both sides of the module through one of the two RX links (though for most barrel modules this necessitates bypassing one of the ABCD chips, leading to the loss of 128 channels from the readout).

In late 2008 and early 2009, TX channels were being lost at an unacceptable rate (the redundancy scheme does not allow recovery of two adjacent modules with TX problems). The suspected cause of this was electrostatic damage to the VCSEL (Vertical Cavity Surface Emitting Laser) arrays on the off-detector transmitters during manufacture. A new batch of TX plugins was ordered and manufactured, with improved electrostatic precautions, and these were installed in July 2009. Since then, three channels have failed, all shortly after installation, consistent with the expected early failure rates.

## 3. Beam splash events

On September 10th 2008, LHC beams 1 and 2 were separately fired into collimators 140m upstream of ATLAS. For the SCT, the first priority was detector safety, in particular with regard to

the risk that large charge deposits on the wafers could damage the ABCD chips. The SCT barrels were therefore turned off for this exercise, while the endcaps were included in the readout, but with a bias voltage of 20V (well below the depletion voltage of 60V). Large numbers of hits and space points were seen in the SCT for these events, as shown in Fig 2, demonstrating that the full readout chain for the SCT was functioning, and that the modules have non-zero hit efficiency even at this much-reduced bias voltage.

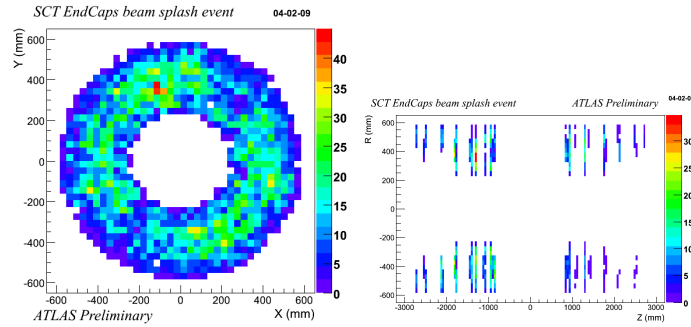


**Figure 2:** Space point distributions for a beam splash event in the SCT endcaps.

## 4. Cosmic ray data

ATLAS recorded significant quantities of cosmic ray data in the periods September-December 2008, and June-November 2009. In total, ATLAS recorded over 3 million tracks with one or more SCT hits during these periods, providing a very useful data sample for detector performance studies.

### 4.1 Single hit efficiency

In order to measure the intrinsic hit efficiency of the SCT, a “holes-on-tracks” method is used to measure the fraction of “hits per possible hit”. Tracks passing through inactive detector regions, wafers giving readout errors, or otherwise excluded from the Data Acquisition, are excluded from the efficiency calculation. Figure 3 shows the average hit efficiency in each barrel layer. The following requirements are made on the hits and tracks that contribute to this plot:

- Cosmic muons with  $\geq 10$  SCT hits and  $\geq 30$  TRT hits,  $\chi^2/\text{DoF} < 2$ .
- Incident angle with wafer  $\leq 40^\circ$  from normal.
- Hits both before and after module under study.
- Guard region around the edge of the active silicon excluded.

The overall hit efficiency for the silicon is found to be 99.75%.

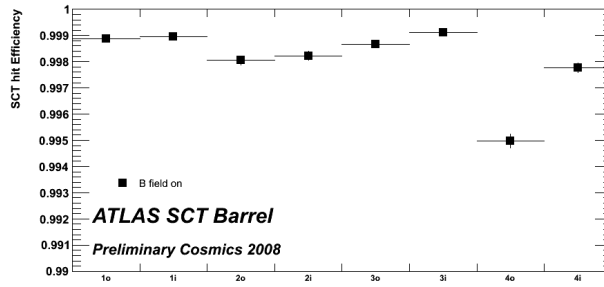


**Figure 3:** Average hit efficiency for each barrel layer and side.

## 4.2 Timing

The SCT reads out three bunch-crossing (25ns) time bins around the “Level 1 Accept” signal. In order to reduce hits from random noise, it is possible to configure the ABCD chips to only accept hits with a “01X” hit pattern (i.e. no hit in the bunch-crossing preceding the Level-1 accept signal, a hit in the same bunch-crossing as the Level-1 accept, and no requirement on whether or not there was a hit in the last of the three bunch-crossings). However, before this readout mode can be activated, it is necessary to “time in” with the Level 1 trigger and other ATLAS subsystems. For this reason, the SCT currently operates in a mode where a hit is accepted if the charge deposited in a strip exceeds the 1fC threshold in any of the three time bins. Delays can be applied module-by-module to the trigger signal to correct for different optical fibre lengths, and for the time-of-flight of particles from the interaction point to the module. The latter correction was first applied in November 2009, and will be fine-tuned further with the first collisions data.

Figure 4 shows the time bin distribution for cosmic tracks. This demonstrates that, having applied the necessary delays to the trigger signal sent to the modules, the SCT is well timed-in.

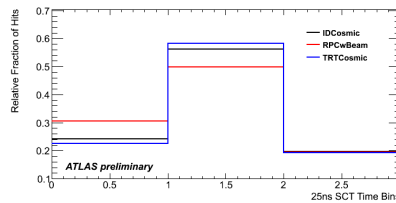


**Figure 4:** Plot showing the time distribution for hits on tracks in 2008 cosmics data. The three bins on the  $x$ -axis represent the three bunch-crossings around the Level 1 Accept signal.

## 4.3 Noise

The design target for noise occupancy of the SCT was  $5 \times 10^{-4}$ . The noise occupancy can be measured either in standalone calibration runs, or in physics runs by looking at random triggers. Both of these are shown in Fig. 5. These results show that the SCT is well within its design parameters, with the expected dependence on strip length.

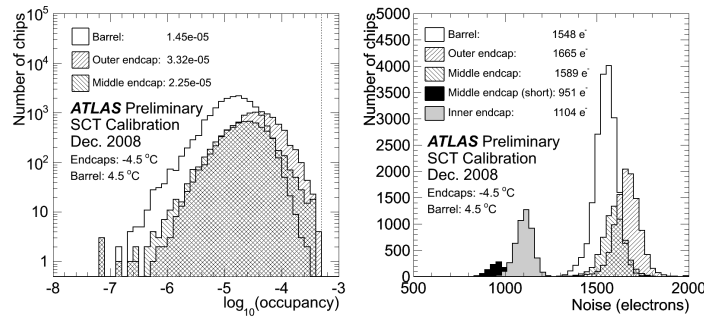


**Figure 5:** The left plot shows the noise occupancy distribution for different types of module, as taken from random triggers in the 2008 cosmic data run. The right plot shows the noise in electron counts, as measured in a standalone calibration test.

### 4.4 Alignment

Cosmic rays are extremely useful in the alignment of the SCT barrels. As the vast majority pass vertically through the detector, they provide more information on alignment in the horizontal (“x”) plane than the vertical, and are also of only limited use for aligning the endcaps. However, the distribution of residuals of hits associated to tracks, after alignment, as shown in Fig. 6, shows that the ideal  $x$  resolution, based on Monte Carlo simulation, is already being approached. Alignment in the  $y$  direction, and of the endcaps, will be dramatically improved with first collisions data.

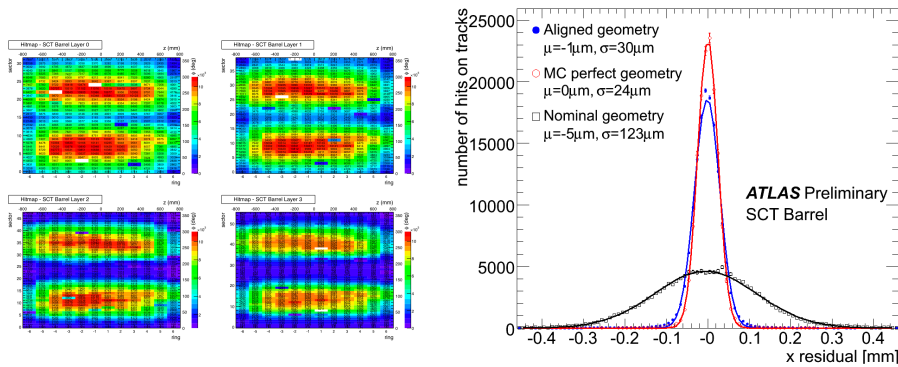


**Figure 6:**  $\eta/\phi$  distribution of tracks used to align the SCT barrel, and  $x$ -residual values before and after alignment.

### 4.5 Lorentz angle

As charge carriers drift through the silicon wafer towards the readout strips, they will be deflected by the presence of a magnetic field. The angular deflection relative to the electric field direction is the *Lorentz* angle, and is a function of magnetic field strength, the bias voltage applied across the wafer, and the temperature (and hence charge carrier mobility).

Figure 7 shows the Lorentz angle measurement on the ATLAS SCT from 2008 cosmics data and also the variation with temperature. The measurement is based on the relationship between

the number of contiguous strips hit (“cluster size”), and the incidence angle of a charged particle track with the wafer. In the absence of a magnetic field, the cluster size would be at a minimum for particles travelling perpendicularly through the wafer. With a B-field present, the average cluster size will still be a minimum for the situation where the charge carriers drift along the direction of the particle track, i.e. the incidence angle of the track is equal to the Lorentz angle. Based on the 2008 cosmic ray data, the Lorentz angle of the SCT barrel was measured to be  $\theta_L = 3.93 \pm 0.03(\text{stat.}) \pm 0.10(\text{sys.})$  degrees, in agreement with the model prediction of  $\theta_L = 3.69 \pm 0.26$  degrees.

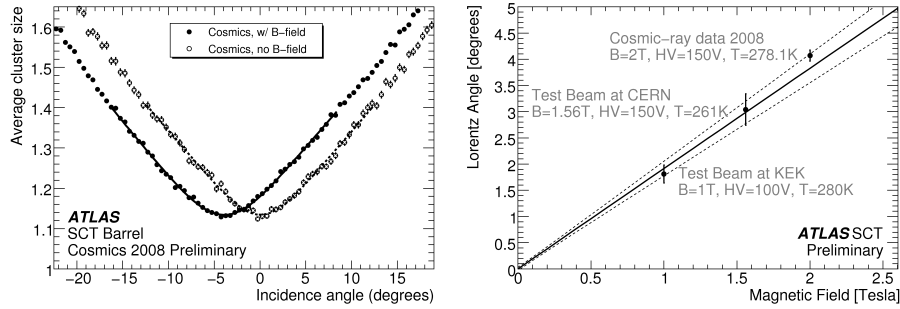


**Figure 7:** The left plot shows the dependence of average cluster width versus incidence angle of the track with respect to the normal to the wafer surface. The offset of the minimum from zero is equal to the Lorentz angle. The right plot shows the temperature dependence of the measured Lorentz angle.

## 5. Conclusions

After many years of preparation and construction prior to its installation in the cavern at CERN, followed by extensive testing and calibration, the operation of the ATLAS Semiconductor Tracker has so far been extremely successful. The hit efficiency and noise levels are better than the design requirements, and the data acquisition, detector controls, and cooling systems are all performing well. Overall, the SCT is on course to be an important and reliable component of the ATLAS detector during the next years of LHC collisions.

## References

- [1] The ATLAS Collaboration, *The ATLAS experiment at the CERN Large Hadron Collider*, JINST 3 (2008) S08003
- [2] ATLAS Inner Detector Technical Design Report, CERN/LHCC97-16 (1997)
- [3] A. Abdesselam et al., *The barrel modules of the ATLAS semiconductor tracker*, Nucl. Instrum. Meth. A568 (2006) 642
- [4] A. Abdesselam et al., *The ATLAS semiconductor tracker end-cap module*, Nucl. Instrum. Meth. A575 (2007) 352
- [5] F. Campabadal et al., *Design and performance of the ABCD3TA ASIC for readout silicon strip in the ATLAS semiconductor tracker*, Nucl. Instrum. Meth. A552 (2005) 561